Marco Wyss*, Mirko Kaiser, Theo Kluter, Tobia Brusa, Martin Bertsch, Volker M. Koch

# The Most Efficient Spectrum for 3D Scanning of Human Skin

## Retrofitting a Standard RGB Projector with Three Wavelength-Shifted Red LEDs

https://doi.org/10.1515/cdbme-2025-0135

**Abstract:** Reflection-based 3D scanning techniques are widely used in medical applications today. In these techniques, encoded light patterns are projected onto the skin, reflected, and captured by 2D cameras. Conventional RGB white-light projectors emit wavelengths that are suboptimal for darker skin types. This results in weakly reflected patterns, prolonged exposures, and increased artefacts in the 3D image. The aim of this project is to optimise an RGB projector for reflection-based 3D scanning of human skin. The methods included evaluating the intensity of reflected patterns and the LED power consumption. A novel concept employing three red LEDs with slightly shifted wavelength peaks was devised and simulated. It exploits the ideal spectrum, while keeping costs and power consumption low.

**Keywords:** 3D body scanning, pattern projector, RGB LED light engine, spectral emission, spectral reflection, human skin reflectance, silicone skin phantoms.

## 1 Introduction

3D scanning is an essential tool in modern medical technology, providing detailed body shape information for applications such as orthodontics, prosthetic design, forensic injury assessment, and the monitoring of scoliosis [1]. Reflection-based 3D scanning techniques are well suited to these applications. In these methods, one or more encoded light patterns are projected onto the skin, reflected, and then captured by at least one 2D camera. Both the wavelength (colour) of the light and the Fitzpatrick skin type (FP 1-6), influence how well the skin reflects these patterns. Additionally, the camera's quantum efficiency determines how effectively each colour of light is captured. Human skin is most reflective in the red to near-infrared spectrum [2]. Ideally, the projected light patterns and the quantum efficiency of the camera should coincide with these spectra.

However, conventional RGB white-light projectors emit green and blue wavelengths that fall outside this range. Especially for darker skin types (FP 3–6), this results in weakly reflected patterns that require prolonged exposure. This increases motion artefacts, ambient light sensitivity, and the risk of incomplete scans due to a low signal-to-noise ratio [3]. Simply using a brighter projector is not a viable solution because this significantly increases both cost and power consumption. The latter considerably limits future integration into mobile 3D scanners, e.g., for scoliosis monitoring [4].

Therefore, this project focuses on optimising a conventional RGB white-light pattern projector for reflection-based 3D scanning of skin without increasing costs or power consumption. Measurements were conducted on human volunteers and silicone phantoms representing the full range of skin types. Subsequently, the RGB LED light engine of the pattern projector was analysed for optimisation potential.

A novel concept using three red LEDs with slightly shifted wavelength peaks was devised and simulated. For a visible light camera, this exploits the most efficient spectral range for human skin.

## 2 Materials and Methods

This project examined how a standard white-light RGB projector light engine, equipped with separate red, green, and blue LEDs, could be optimised for pattern projection on human skin. The aim was to achieve the maximum captured pattern intensity with the minimum electrical power consumption (max. efficiency). Therefore, the efficiency for reflection-based 3D scanning was introduced as the measure of performance. It was defined as the ratio of captured pattern intensity (output) to electrical power consumption (input).

Thus, the electrical power consumption of each LED was measured with a digital oscilloscope. The associated pattern intensity was calculated based on the obtained camera images.

***Marco Wyss, Tobia Brusa, Theo Kluter, Volker Koch:** Institute for Human-Centered Engineering, Bern University of Applied Sciences, Quellgasse 21, 2502 Biel/Bienne, Switzerland *marco.wyss@bfh.ch
**Martin Bertsch, Mirko Kaiser:** Laboratory for Movement Biomechanics, ETH Zurich, 8092 Zürich, Switzerland

Eight volunteers (FP 2 to 6) and three silicone skin phantoms were tested (FP 1, 3, and 6). The phantoms, mimicking the spectral reflectance of different Fitzpatrick skin types 1, 3, and 6, were fabricated for consistent measurements. To achieve a non-shiny, skin-like surface, the silicone had to be cast onto a slightly rough surface (Biloxit 100 sandblasted aluminium). The skin phantoms were validated by comparing the spectral reflectance with those of the volunteers. The maximum deviations observed (−4.7 % to +6.5 %) were within acceptable limits for this project.

All eleven measurements were performed in a controlled indoor environment with excluded sun and ambient light. The materials available for the experiments are listed hereafter:

- Projector: Texas Instruments, DLPLCR4500EVM
  - Light engine: iView Limited, IPD1231G
- Camera: Thorlabs, CS505MU
- Spectrometer: Ocean Optics, STS-VIS
- Oscilloscope: R&S, RTM3004
  - Differential voltage probe: R&S, RT-ZD10
  - Voltage probe attenuator: R&S, RT-ZA15
  - Current clamp: R&S, RT-ZC31
- Silicone: SpectroMATCH, Reality Series LSR (M511)
  - Lightest European colour (FP 1): A-Nr. 1.1
  - Medium light European colour (FP 3): A-Nr. 1.3
  - Darkest Caucasian colour (FP 6): A-Nr. 3.4

## 2.1 Examining the light engine's performance

The performance of the RGB LED light engine itself partly determines the overall efficiency. It converts electrical power into light using a red, green and blue LED. Consequently, the performance of each LED must be assessed individually.

To do so, the electrical power consumption $P_{el}$ in Watt of each LED was measured with the digital oscilloscope. At the same time, the spectrometer was used to measure the projected light spectrum $S_{proj}$. The radiant power $\Phi$ in Watt was then derived by integration of $S_{proj}$.

From these data, the light engines efficiency $\eta_{LED}$ in converting electrical power into radiant power was derived for each colour (red, green, blue, and white) (eq 1).

$$\boldsymbol{\eta_{LED}} = \frac{\boldsymbol{\Phi}}{\boldsymbol{P_{el}}} = \frac{\int(\boldsymbol{S_{proj}})}{\boldsymbol{P_{el}}} \tag{1}$$

## 2.2 Examining the pattern intensity

The pattern intensity $I_{cap}$ was determined from the captured images $I_{2D}$ (eq 2). A series of red, green, blue, and white light was projected onto the volunteer's skin or silicone phantom and photographed with the camera. The monochrome camera generates greyscale images with a specific brightness for each colour. Ambient light was excluded to measure only reflected projector light. The camera exposure time was kept constant within a series, allowing comparison.

In addition, the reflected light patterns $S_{refl}$ were collected with a spectrometer. Thus, the theoretically expected pattern intensity could be calculated for each colour. This was done by multiplying the spectral intensity curve of the reflected light $S_{refl}$ with the camera's spectral sensitivity curve QE (quantum efficiency). The area under the resulting curve corresponded to the light power received by the camera. The theoretical pattern intensity $I_{sim}$ was then calculated by integration (eq 3).

$$\boldsymbol{I_{cap}} = \boldsymbol{mean(I_{2D})} \tag{2}$$

$$\boldsymbol{I_{sim}} = \int\left(\boldsymbol{S_{refl}} \cdot \boldsymbol{QE}\right) \tag{3}$$

## 2.3 Deriving the efficiency for reflection-based 3D scanning

As introduced as measure of performance, the efficiency $\eta_{cap}$ was calculated by dividing the captured pattern intensity $I_{cap}$ by the measured electrical power $P_{el}$ of the LEDs (eq 4).

Additionally, the spectrometer measurements of the reflected light $S_{refl}$, combined with the camera's quantum efficiency QE and the LED power consumptions $P_{el}$, enabled the calculation of the expected efficiency $\eta_{sim}$ for each colour (eq 5). These calculations were used to verify the camera-based measurements. They also formed the basis for subsequent optimisation simulations.

$$\boldsymbol{\eta_{cap}} = \frac{\boldsymbol{I_{cap}}}{\boldsymbol{P_{el}}} = \frac{\boldsymbol{mean(I_{2D})}}{\boldsymbol{P_{el}}} \tag{4}$$

$$\boldsymbol{\eta_{sim}} = \frac{\boldsymbol{I_{sim}}}{\boldsymbol{P_{el}}} = \frac{\int(\boldsymbol{S_{refl}} \cdot \boldsymbol{QE})}{\boldsymbol{P_{el}}} \tag{5}$$

## 2.4 Towards pattern projection in the optimal wavelength range

While the spectral reflection of the human skin is given, the pattern projector and the 2D camera can be chosen, or even customized. As introduced, projector and camera ideally align to the best spectral reflectance of human skin (FP 1 = 600–1130 nm, FP 6 = 800–1135 nm).

However, conventional 2D cameras are made for the visible wavelength range (400-750 nm) with decreasing sensitivity above approx. 600 nm. On the other hand, comparable cameras with increased sensitivity in the near-infrared range (750-1500 nm) are significantly more

expensive. These were out of the question in the search for cost-neutral solutions.

The ideal spectrum $S_{ideal}$ for pattern projection was then found by multiplying the skin's spectral reflectance R with the camera's quantum efficiency QE (eq 6) (Figure 1) [2].

$$S_{ideal} = R \cdot QE \quad (6)$$

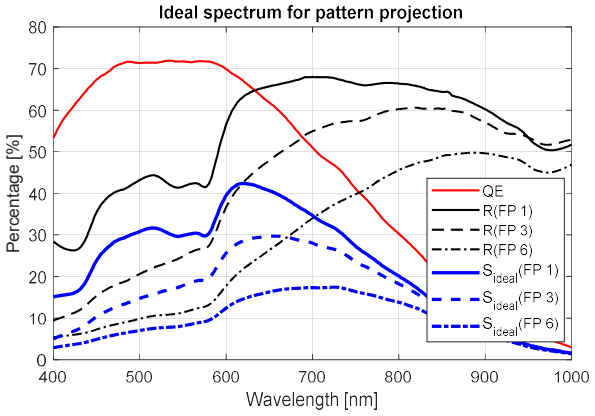


**Figure 1:** The ideal spectrum $S_{ideal}$ for pattern projection on to human skin is shown for the lightest skin tone (FP 1), for the medium light (FP 3), and the darkest (FP 6). These spectra are based on the camera's quantum efficiency QE and the reflectance of different skin tones R(FP 1, 3, and 6) [2].

# 3 Results

## 3.1 Performance of the light engine

The radiant power Φ of the green LED (2.88 W) surpassed that of the blue (2.38 W) and red (1.31 W). Combined, these produced the white light (6.57 W).

However, the LED's electrical power $P_{el}$ consumption was highest for green (9.1 W), higher than that of the blue (8.3 W) and the red LED (5.1 W). Combined, this was the power consumption for white light (22.5 W).

The efficiency $\eta_{LED}$ (eq 1) of the green LED (31.6 %) surpassed both the blue (28.8 %) and the red (26.6 %). Combined, this was the efficiency for white light (29.2 %).

## 3.2 Pattern intensity

The results for $I_{cap}$ are expressed as mean values (μ) and standard deviations (σ). For all eight volunteers, compared to normalised white light ($\mu_w$ = 100 %, $\sigma_w$ = 0.0 %), green produced on average the highest relative pattern intensity ($\mu_g$ = 38.7 %, $\sigma_g$ = 1.2 %), compared to the red ($\mu_r$ = 36.0 %, $\sigma_r$ = 1.6 %) and blue ($\mu_b$ = 25.3 %, $\sigma_b$ = 1.7 %) (Figure 2, left).

And similar for the silicone phantoms, green produced on average the highest relative pattern intensity ($\mu_g$ = 40.0 %, $\sigma_g$ = 1.0 %), compared to the red ($\mu_r$ = 28.4 %, $\sigma_r$ = 4.3 %) and blue LED ($\mu_b$ = 31.6 %, $\sigma_b$ = 3.5 %) (Figure 2, right).

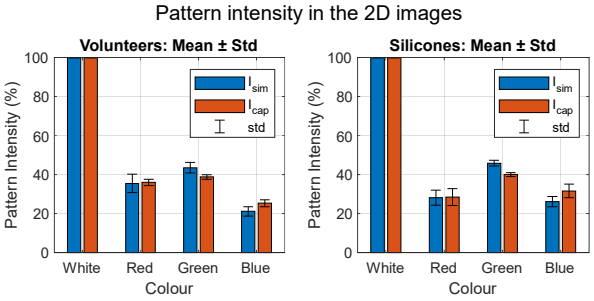


**Figure 2: Left)** These are the captured and simulated relative pattern intensities of all eight volunteers for each projected colour. **Right)** In comparison, the relative pattern intensity of the silicone skin phantoms.

## 3.3 Derived efficiency for reflection-based 3D scanning of skin

The results for $\eta_{cap}$ are expressed as mean values (μ) and standard deviations (σ). For all eight volunteers, compared to the normalised efficiency of white light ($\mu_w$ = 100 %, $\sigma_w$ = 0 %), the efficiency of red was always highest ($\mu_r$ = 168.6 %, $\sigma_r$ = 7.5 %), compared to green ($\mu_g$ = 97.9 %, $\sigma_g$ = 3.0 %), and blue ($\mu_b$ = 70.2 %, $\sigma_b$ = 4.8 %) (Figure 3, left).

And similar for the silicones skin phantoms, compared to the normalised efficiency of white light ($\mu_w$ = 100 %, $\sigma_w$ = 0 %), the efficiency of red was always highest ($\mu_r$ = 133.3 %, $\sigma_r$ = 20.1 %), compared to green ($\mu_g$ = 101.1 %, $\sigma_g$ = 2.4 %), and blue ($\mu_b$ = 87.8 %, $\sigma_b$ = 9.7 %) (Figure 3, right).

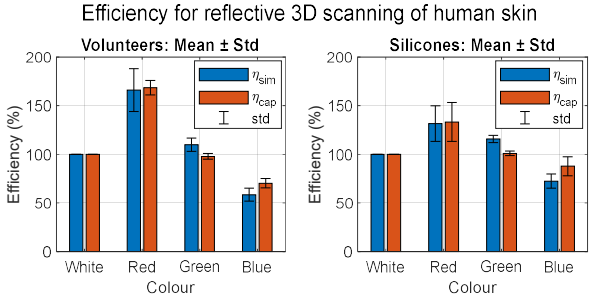


**Figure 3: Left)** The efficiency for reflective 3D scanning of volunteers for each projected colour. Derived of the pattern intensity divided by the electrical power consumption. **Right)** In comparison, the efficiency for the silicone skin phantoms.

### 3.4 Optimised projector light for human skin's spectral reflectance

The proposed light engine retrofit combines three red LEDs with slightly different wavelength peaks (640 nm, 702 nm, and 764 nm). This can be observed in the simulated projected light spectrum $S_{proj}$(3WSR light) (Figure 5). The darkest skin type (FP 6) has the lowest reflectance R and ideal spectrum $S_{ideal}$. This makes it the most difficult skin type to measure [3]. The 3WSR light was therefore optimised for this skin type.

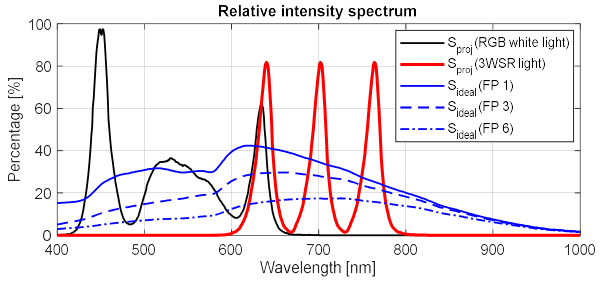


**Figure 4:** Due to the low reflectance, the darkest skin tone (FP 6) requires longest exposure times and most improvement. Hence, the 3WSR light was tuned to the ideal spectrum (640-764 nm) for this skin tone.

Since the white and 3WSR lights have the same power consumption (22.5 W), the normalised pattern intensity $I_{sim}$ (Figure 5, left) is equal to the normalised efficiency $\eta_{cap}$ (Figure 5, right). Compared to normalised white light, the 3WSR light generates a lower pattern intensity and is less efficient for very light skin types (FP 1) (86.7 %). For medium skin types (FP 3), the 3WSR light generates higher pattern intensity and is more efficient (119.7 %). For dark skin types (FP 6), which require improved pattern projection, the 3WSR light generates significantly higher pattern intensity and is significantly more efficient (149.3 %).

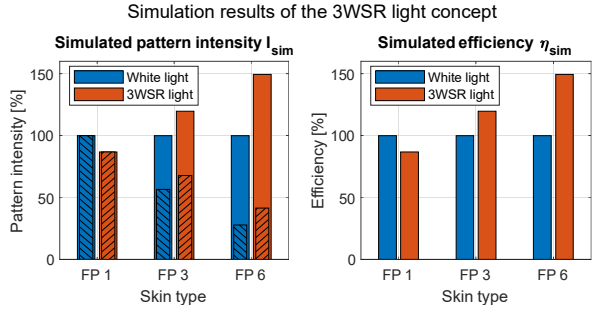


**Figure 5: Left)** Simulated relative pattern intensities for the lightest, middle, and darkest skin tone (FP 1, 3, and 6). Once compared to normalised white light of FP 1, 3, and 6. Once compared to normalised white light of FP 1 (highlighted with stripes). **Right)** Simulated efficiency for reflective 3D scanning of human skin.

# 4 Conclusion

The main goal of this project was to optimise an RGB white-light projector for reflection-based 3D scanning of human skin. This, without increasing cost or power consumption. Tests on volunteers and silicone phantoms demonstrated that conventional RGB white-light projection is suboptimal for darker skin types. The simulated pattern intensity in 2D images and the corresponding scanning efficiency both confirmed that standard RGB white light does not fully leverage the higher reflectance of skin in the red to near-infrared range. The measurements validated these findings.

The simulation of the proposed three wavelength-shifted red LED concept (3WSR) shows notably increased captured pattern intensity and scanning efficiency, especially for darker skin types. At the same time, it only requires minimal hardware modifications.

The improvement was limited by the camera's diminishing quantum efficiency beyond 600 nm. Additionally, the inferior performance of the red LEDs in converting electrical into radiant power restricted performance.

The 3WSR concept offers less benefit for very light skin. However, it excels at darker skin types that are otherwise difficult to measure. This ensures dependable medical 3D scanning across all skin types.


#### Author Statement

Research funding: Innosuisse grant (47195.1 IP-LS).
Conflict of interest: Authors state no conflict of interest.
Informed consent: Obtained from all volunteers.
Ethical approval: Ethics committee BFH, Nr. EAB2022_018.


## References


[1] A. T. D. Grünwald, S. Roy, and R. Lampe, "Scoliosis assessment tools to reduce follow-up X-rays," *J Orthop Translat*, vol. 38, pp. 12–22, Jan. 2023, doi: 10.1016/J.JOT.2022.07.010.

[2] T. Kono and J. Yamada, "In Vivo Measurement of Optical Properties of Human Skin for 450–800 nm and 950-1600 nm Wavelengths," *Int J Thermophys*, vol. 40, no. 5, p. 51, May 2019, doi: 10.1007/s10765019-2515-3.

[3] I. Brintouch, A. Ali, G. E. Romanos, and R. A. Delgado-Ruiz, "Influence of Simulated Skin Color on the Accuracy of Face Scans," *Prosthesis 2024,* vol. 6, pp. 1372-1382, Nov. 2024, doi: 10.3390/PROSTHESIS6060099.

[4] Y. Oquendo *et al.*, "Mobile device-based 3D scanning is superior to scoliometer in assessment of adolescent idiopathic scoliosis," *Spine Deform*, vol. 13, pp. 529-537, Dec. 2024, doi: 10.1007/s43390-024-01007-6.